Journal of Sound and Vibration (2000) **236**(4), 575–594
doi:10.1006/jsvi.2000.2994, available online at http://www.idealibrary.com on IDEAL®

THE TRANSFER MATRIX FOR A DISSIPATIVE SILENCER OF ARBITRARY CROSS-SECTION

R. GLAV

The Marcus Wallenberg Laboratory for Sound and Vibration Research, Department of Vehicle Engineering, Royal Institute of Technology, S-10044 Stockholm, Sweden

(*Received* 21 *September* 1999, *and in final form* 31 *January* 2000)

In this work, the acoustic transfer matrix for a cylindrical dissipative silencer of arbitrary cross-section and bulk-reacting lining is derived for the case of negligible mean flow. The derivation is performed in a two-step procedure. First, the corresponding infinite-lined duct is analyzed by separating the longitudinal dependence and using collocation for the entailing eigenvalue problem. Then, using the resulting eigenmodes, the acoustic field in the silencer is expanded and adjusted to the boundary conditions at the in/outlet by mode-matching. To illustrate the applicability and numerical efficiency of the proposed technique a practical example is given.

1. INTRODUCTION

One of the most common types of silencer in practical flow duct acoustics is the cylindrical dissipative silencer. This combines large mid- and high-frequency attenuation with low back pressure and it is also, with its typically quite non-reactive acoustical behaviour, comparably easy to combine with other silencers in, e.g., an automative exhaust system or a ventilation duct. The major drawbacks are the poor low-frequency attenuation and the erosion and clogging of the porous material packed within the silencer. It is also difficult to model accurately and efficient optimization is thus not an easy task. The modelling difficulties are due to a number of reasons, one being the description of the porous material, another being the analysis of the acoustic field in the silencer. For higher Mach numbers, flow-acoustic effects may also impede the modelling.

The attempts to model the cylindrical dissipative silencer may be classified by whether the lining is assumed to be locally-or bulk-reacting. The former case has been treated frequently, in the literature, where the work by Morse [1] in 1939 may serve as a foundation. The bulk-reacting case has not been discussed to the same extent even though an analysis of the sound field inside both a two-dimensional (2-D) rectangular lined duct as well as a circular lined duct (omitting any angular variation) was presented by Scott [2] as early as 1946. This analysis is however, like most more recent contributions regarding dissipative silencers with bulk-reacting lining, concerned only with the infinite case, i.e., all inlet and outlet effects associated with an actual, finite silencer are omitted. If the lining is acoustically dense, the results may, as will be illustrated below, still be useful in practice but as many applications require a lighter absorbent to obtain the desired attentuation, a more complete analysis is needed. Such an analysis, using Wiener–Hopf technique, was first presented by Nilsson and Brander [3] in 1980, concerning a silencer with a superimposed mean flow in the central passage. In 1988, Cummings and Chang [4], by use of straightforward mode-matching

0022-460X/00/390575 + 20 $35.00/0

technique, analyzed a similar device including mean flow effects also within the lining. Based on this work, a transfer matrix formulation for the bulk-reacting dissipative silencer was developed by Peat [5]. Both these latter contributions, as well as the earlier papers by Nilsson and Brander, are restricted to the case of circular cross-section. In a practical application where the outer shape is in many cases decisive for the choice of design, this apparently reduces the applicability of these models. Moreover, as the geometry is also assumed to be axisymmetric, i.e., concentric inlet/outlet, only radially dependent modes are included in the analysis. A completely arbitrary geometry, neglecting mean flow, has been addressed by Tarnow and Pommer [6] using a Green's function technique. They did not however present any complete technique to obtain the appropriate Green's function in the more general case. Quite recently, Peat and Rathi [7] have presented what seems to be the most complete modelling of a dissipative silencer so far, including both mean flow and complex geometry as well as anisotropy of the liner. However, as it is a full 3-D FEM approach, the numerical effort may be considerable and limits the usefulness in an iterative design process.

The purpose of this work is to extend the modelling capabilities concerning cylindrical dissipative silencers by deriving the plane wave transfer matrix, i.e., the most common formulation in the acoustic 2-port method, for a silencer with arbitrary cross-section and inlet/outlet location. To simplify the analysis, and also because a number of important applications typically have Mach numbers less than 0·1, (for instance, the automotive exhaust system), mean flow is neglected. The governing equations and boundary/coupling conditions for this problem are formulated below in section 2 whereas the actual derivation is given in section 3. To obtain a numerically efficient formulation, the cylindrical feature of the problem is utilised, and thus the derivation may be performed in a two-step procedure. First, the eigenmodes of the corresponding infinite-lined duct are determined using the technique of collocation and, second, mode matching is employed to include the longitudinal boundary and coupling conditions. Schematically, there are some similarities with the technique of Cummings and Chang [4] although 3-D waves are now included both in the lined duct as well as in the inlet/outlet. In section 4, the various numerical solvers used in the computer coding are summarized and some numerical results from the analysis of a realistic automotive silencer are presented. Finally, in section 5, the work is summarized and some conclusions are drawn.

2. FORMULATION OF THE PROBLEM

A cylindrical dissipative silencer is suitably divided into four regions; inlet, outlet, central passage and lining (Figure 1). The first three convey the gases, e.g., air or IC-engine exhaust gases, whereas the lining is included only for the sake of noise control. The geometry is most conveniently represented in a cylindrical co-ordinate system with the z-axis directed along the main axis, thus enabling the cross-sectional dimensions to be given by the parametric curves $\Gamma_1{:}r = a(\varphi)$ and $\Gamma_2{:}r = b(\varphi)$. As seen from Figure 1, the cross-section of the central passage, S_1, is assumed to fit precisely the cross-sections of the inlet and outlet regions. From a modelling point of view this is not decisive although simplifying, but is instead imposed by the fact that most dissipative silencers are manufactured from a perforated tube wrapped by porous materials, thus having the appearance illustrated. In an application of considerable mean flow, such a design also helps to reduce the static pressure drop. In addition to guiding the mean flow, the perforated shielding will also protect the porous material from erosion. As the open area of the perforations is typically well above 20%, the acoustic effects however, are usually very small and will thus be neglected below.

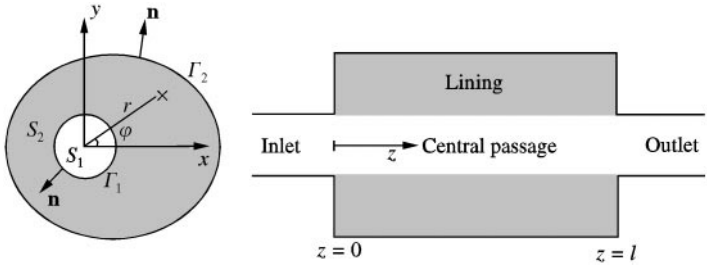

Figure 1. The geometry of a cylindrical dissipative silencer.

Consider a stationary problem, the time-factor $\exp(-i\omega t)$ is omitted below, and assume the medium in each region to be homogenous, quiescent and isotropic. By also assuming linear acoustics, the Helmholtz equation is valid for the acoustic velocity potential, defined from $\mathbf{v} = -\nabla\Psi$, in each region,

$$\nabla^2\Psi_1 + k_1^2\Psi_1 = 0, \quad \text{central passage}, \tag{1}$$

$$\nabla^2\Psi_2 + k_2^2\Psi_2 = 0, \quad \text{lining}, \tag{2}$$

$$\nabla^2\Psi_3 + k_1^2\Psi_3 = 0, \quad \text{inlet}, \tag{3}$$

$$\nabla^2\Psi_4 + k_1^2\Psi_4 = 0, \quad \text{outlet}. \tag{4}$$

Here ∇ denotes the three-dimensional nabla operator in cylindrical co-ordinates $(\mathbf{e}_r, \mathbf{e}_\varphi, \mathbf{e}_z)$,

$$\nabla = \mathbf{e}_r\frac{\partial}{\partial r} + \mathbf{e}_\varphi\frac{1}{r}\frac{\partial}{\partial\varphi} + \mathbf{e}_z\frac{\partial}{\partial z}, \tag{5}$$

and $k_{1,2} = \omega/c_{1,2}$ the wavenumber. In those regions that convey the gases, the medium is assumed to be non-dissipative and the density and sound velocity, denoted ρ_1 and c_1 respectively, thus have real values in the frequency domain. Inside the lining on the other hand, the bulk-reacting mixture of porous material and gases is, by definition, dissipative and ρ_2 and c_2 have complex values with, as long as the resulting solutions are causal, an optional frequency dependence.

By regarding all envelope surfaces as rigid, the boundary conditions for the different regions are

$$\nabla\Psi_2 \cdot \mathbf{n}|_{r=b} = 0, \quad 0 < z < \ell, \tag{6}$$

$$\nabla\Psi_3 \cdot \mathbf{n}|_{r=a} = 0, \quad z \leqslant 0, \tag{7}$$

$$\nabla\Psi_4 \cdot \mathbf{n}|_{r=a} = 0, \quad z \geqslant \ell, \tag{8}$$

$$\left.\frac{\partial\Psi_2}{\partial z}\right|_{z=0,\ell} = 0, \quad (r, \varphi) \in S_2, \tag{9}$$

where the last condition is obtained from the rigid endplates of the silencer. The normal vector **n** is defined in Figure 1. As can be seen the central passage is not directly involved in any of these conditions but is instead affected by the requirements for continuity in acoustic pressure and normal velocity across the boundaries between the different regions. Thus, the following coupling conditions are valid for the gas conveying regions;

$$\Psi_1(r, \varphi, 0) = \Psi_3(r, \varphi, 0), \quad (r, \varphi) \in S_1, \tag{10}$$

$$\Psi_1(r, \varphi, \ell) = \Psi_4(r, \varphi, \ell), \quad (r, \varphi) \in S_1, \tag{11}$$

$$\left.\frac{\partial \Psi_1}{\partial z}\right|_{z=0} = \left.\frac{\partial \Psi_3}{\partial z}\right|_{z=0}, \quad (r, \varphi) \in S_1, \tag{12}$$

$$\left.\frac{\partial \Psi_1}{\partial z}\right|_{z=\ell} = \left.\frac{\partial \Psi_4}{\partial z}\right|_{z=\ell}, \quad (r, \varphi) \in S_1, \tag{13}$$

and the lining,

$$\rho_1 \Psi_1(a, \varphi, z) = \rho_2 \Psi_2(a, \varphi, z), \quad 0 < z < \ell, \tag{14}$$

$$\nabla \Psi_1 \cdot \mathbf{n}|_{r=a} = \nabla \Psi_2 \cdot \mathbf{n}|_{r=a}, \quad 0 < z < \ell. \tag{15}$$

Finally, all involved fields and their derviatives must be periodic concerning the polar angle,

$$\left.\frac{\partial^n \Psi_p}{\partial \varphi^n}\right|_{\varphi} = \left.\frac{\partial^n \Psi_p}{\partial \varphi^n}\right|_{\varphi \pm m2\pi}, \quad p = 1, 2, 3, 4, m = 1, 2, \ldots, n = 0, 1. \tag{16}$$

It should also be observed that in this problem there are geometrical singularities at $r = a$, $z = 0$ and $r = a$, $z = \ell$. To handle these, a so-called "edge condition" [8] may be imposed. This requires the acoustical energy contained within a vanishing volume enclosing the singularity to be finite and it will also warrant an unique solution of the field.

As this work is concerned with the transfer matrix description of the dissipative silencer, only plane waves are allowed to propagate in the inlet and outlet regions and, as a consequence, the maximum cross-sectional dimension of these regions is, for a given frequency, restricted. Furthermore, as the main objective, underlying not only the transfer matrix method but all building block techniques, is to obtain a description of each subsystem that is independent of the rest of the system, no evanescent higher order modes may be incident upon the dissipative section and thus the inlet and outlet ducts are assumed to be "long enough".

3. DERIVATION OF THE TRANSFER MATRIX

The most straightforward method of solving the problem formulated above, especially considering the cylindrical geometry, is probably to use the technique of *mode-matching* [8].

By this method, the problem is, partly as a consequence of its transmission line feature, most suitably separated into three parts along the z-axis; inlet, outlet and lined duct, the last part being a combination of the central passage and the lining. Each of these parts is then analyzed separately for a case with no z-dependent boundary conditions, i.e., being considered as an infinite duct. This approach will yield the eigenmodes of the different parts and provided these functions constitute a complete set on the corresponding cross-section, all possible fields within each part of the silencer can be represented by combinations of them. The description of the total field is then obtained by matching these partial fields using the longitudinal coupling and boundary conditions.

3.1. THE EIGENMODES

Once the z dependence has been separated by spatial Fourier transformation; $\psi(k_z) = \int_{-\infty}^{+\infty} \Psi(z) \exp(-\mathrm{i}k_z z)\,\mathrm{d}z$ the derivation of the eigenmodes consists of solving two 2-D eigenvalue problems, one for the inlet/outlet and one for the lined duct. By restricting the analysis to applications where the inner cross-section S_1 is circular, separation of variables may be pursued to solve the inlet/outlet problem yielding the well-known modal amplitudes of a cylindrical circular rigid duct,

$$\psi_3^{(q)} = \psi_4^{(q)} = \phi^{(q)} = \mathrm{J}_n(k_r^{(q)} r) \begin{Bmatrix} \cos n\varphi \\ \sin n\varphi \end{Bmatrix}, \tag{17}$$

where the order of the Bessel and the trigonometric functions, n, are integer functions of the eigenmode numbering, q. The modes are numbered according to their cut-on frequency denoting the fundamental no. 1. For the degenerate cases, i.e., for $n > 0$, the cosine angular dependence precedes the sine dependence. The same convention will be used also for the dissipative duct, although referring to the cut-on-frequencies of the corresponding lossless case. The radial wavenumbers $k_r^{(q)}$, which may readily be found in any mathematical handbook [9], are related to the longitudinal wavenumber $k_{z\phi}^{(q)}$ by

$$(k_r^{(q)})^2 = (k_1^{(q)})^2 - (k_{z\phi}^{(q)})^2. \tag{18}$$

The lined duct, on the other hand, generally has a cross-sectional shape which does not lend itself to further separation and instead some more general technique is required. Considering the usually regular cross-sectional shape of the commerical dissipative silencer a natural choice is the simplest possible; *collocation*. This technique has been applied to lined ducts by the author in an earlier work [10] and will therefore only be outlined here for reference purposes. The basic idea is to assume that the modal amplitudes in the lined duct can be approximated by a finite expansion in the polar eigenfunctions. This ansatz is then matched pointwise to the boundary conditions. Thus for the central passage,

$$\psi_1^{(s)} = \sum_{m=0}^{M} \mathrm{J}_m(k_{\perp 1}^{(s)} r)(A_m^{(s)} \cos m\varphi + B_m^{(s)} \sin m\varphi), \tag{19}$$

where s in accordance with equation (17) denotes the eigenmode number and J_m the Bessel function of order m. The Neumann function, denoted N_m below, has been excluded from the

expansion due to its singularity at $r = 0$. A similar ansatz may also be formulated for the modal amplitude in the lining,

$$\psi_2^{(s)} = \sum_{m=0}^{M} \{\mathrm{J}_m(k_{\perp 2}^{(s)} r)(C_m^{(s)} \cos m\varphi + D_m^{(s)} \sin m\varphi),$$

$$+ \mathrm{N}_m^{(s)}(k_{\perp 2}^{(s)} r)(E_m^{(s)} \cos m\varphi + F_m^{(s)} \sin m\varphi)\}. \tag{20}$$

As each term in these two expansions is an exact solution to the governing equations in the eigenvalue problem of the lined duct, the transverse wavenumbers,

$$(k_{\perp 1}^{(s)})^2 = (k_1^{(s)})^2 - (k_{z\psi}^{(s)})^2,$$

$$(k_{\perp 2}^{(s)})^2 = (k_2^{(s)})^2 - (k_{z\psi}^{(s)})^2, \tag{21}$$

as well as the coefficients $A_m^{(s)} - F_m^{(s)}$ are to be determined solely from the boundary conditions (6) and (14), (15). It should be noted that the finite expansions above are of equal length, M. This is a direct consequence of the uniqueness of the Fourier series and the restriction to a circular inner region. By this, the continuity requirements on pressure and normal velocity may be termwise fulfilled and embedded in the formulation. Collocation is accordingly performed using only the rigid-wall boundary condition at Γ_2, giving the following system of linear equations for the coefficients in the modal amplitude expansion in the central passage:

$$\sum_{m=0}^{M} A_m^{(s)} \{k_{\perp 2}^{(s)}(K_{1,m}^{(s)} \mathrm{J}'_m(k_{\perp 2}^{(s)} b_j) + K_{2,m}^{(s)} \mathrm{N}'_m(k_{\perp 2}^{(s)} b_j)) \cos m\varphi_j$$

$$+ \frac{mb'_j}{b_j^2}(K_{1,m}^{(s)} \mathrm{J}_m(k_{\perp 2}^{(s)} b_j) + K_{2,m}^{(s)} \mathrm{N}_m(k_{\perp 2}^{(s)} b_j)) \sin m\varphi_j\}$$

$$+ \sum_{n=0}^{M} B_m^{(s)} \{k_{\perp 2}^{(s)}(K_{1,m}^{(s)} \mathrm{J}'_m(k_{\perp 2}^{(s)} b_j) + K_{2,m}^{(s)} \mathrm{N}'_m(k_{\perp 2}^{(s)} b_j)) \sin m\varphi_j \tag{22}$$

$$- \frac{mb'_j}{b_j^2}(K_{1,m}^{(s)} \mathrm{J}_m(k_{\perp 2}^{(s)} b_j) + K_{2,m}^{(s)} \mathrm{N}_m(k_{\perp 2}^{(s)} b_j)) \cos m\varphi_j\} = 0, \quad j = 1, 2, \ldots, 2M + 1,$$

where prime denotes derivation, $b_j = b(\varphi_j)$ are the points selected for the collocation and, using a well-known relation for Bessel functions [9],

$$K_{1,m}^{(s)} = \frac{\pi a}{2\rho_2}(\rho_1 k_{\perp 2}^{(s)} \mathrm{J}_m(k_{\perp 1}^{(s)} a) \mathrm{N}'_m(k_{\perp 2}^{(s)} a) - \rho_2 k_{\perp 1}^{(s)} \mathrm{J}'_m(k_{\perp 1}^{(s)} a) \mathrm{N}_m(k_{\perp 2}^{(s)} a)), \tag{23}$$

$$K_{2,m}^{(s)} = \frac{\pi a}{2\rho_2}(\rho_2 k_{\perp 1}^{(s)} \mathrm{J}'_m(k_{\perp 1}^{(s)} a) \mathrm{J}_m(k_{\perp 2}^{(s)} a) - \rho_1 k_{\perp 2}^{(s)} \mathrm{J}_m(k_{\perp 1}^{(s)} a) \mathrm{J}'_m(k_{\perp 2}^{(s)} a)). \tag{24}$$

The above equations may be written in matrix form,

$$\mathbf{S} \cdot (A_0^{(s)}, A_1^{(s)}, B_1^{(s)}, \ldots, A_M^{(s)}, B_M^{(s)})^{\mathrm{T}} = \mathbf{0}, \tag{25}$$

where $\mathbf{S}$ apparently has the dimension $(2M+1)\times(2M+1)$ and for the sake of non-trivial solutions, a determinant equal to zero,

$$\det \mathbf{S}(k_{\perp 1}^{(s)}) = 0. \tag{26}$$

From equation (26), which together with equation (21) constitutes the dispersion relation for the lined duct, it is seen that the transversal wavenumber of the central passage, $k_{\perp 1}^{(s)}$, has been chosen as independent variable. This choice is motivated by the assumption that this wavenumber varies the least with frequency and it will consquently facilitate the numerical handling. Once equation (26) is solved the modal amplitude coefficients in the central passage may be calculated from equation (25) and from these, the coefficients for the lining can be evaluated directly,

$$\begin{aligned} C_m^{(s)} &= K_{1,m}^{(s)} A_m^{(s)}, \quad D_m^{(s)} = K_{1,m}^{(s)} B_m^{(s)}, \\ E_m^{(s)} &= K_{2,m}^{(s)} A_m^{(s)}, \quad F_m^{(s)} = K_{2,m}^{(s)} B_m^{(s)}. \end{aligned} \tag{27}$$

Clearly, the eigenmodes of the lined duct are now fully determined but before proceeding to handling the actual finite dissipative silencer some comments may be made upon the collocation technique. Obviously, the simplicity of the collocation technique is very tractable and both derivation and numerical implementation is most straightforward. The major drawback is the dependence of the rate of convergence on the choice of points in the collocation. In contrast to any technique based upon a weak formulation which averages the characteristics of a given problem, collocation performs a discrete sampling and input data is thus geometrically low-pass filtered. In this application, where collocation is performed using a homogeneous condition along a regular and by the trial functions well-captured boundary, the rate of convergence and accuracy will in most cases be reasonable if the angle between consequent collocation points is simply kept constant. However, to improve the results and also avoid possible occurrences of Runge's phenomena for large values of M, an adaptive scheme for the collocation points [10] is utilized here.

3.2. THE MODE MATCHING

Once the eigenmodes and corresponding wavenumbers are known, the actual finite dissipative silencer with inlet and outlet can be analyzed using the technique of mode matching. Initially, the velocity potential in the different regions is formulated as a sum of the corresponding eigenmodes,

$$\Psi_1 = \sum_{s=1}^{S} b_+^{(s)} \psi_1^{(s)} \exp(\mathrm{i}k_{z\psi}^{(s)} z) + \sum_{s=1}^{S} b_-^{(s)} \psi_1^{(s)} \exp(-\mathrm{i}k_{z\psi}^{(s)}(z-\ell)), \quad \text{central passage,} \tag{28}$$

$$\Psi_2 = \sum_{s=1}^{S} b_+^{(s)} \psi_2^{(s)} \exp(\mathrm{i}k_{z\psi}^{(s)} z) + \sum_{s=1}^{S} b_-^{(s)} \psi_2^{(s)} \exp(-\mathrm{i}k_{z\psi}^{(s)}(z-\ell)), \quad \text{lining,} \tag{29}$$

$$\Psi_3 = a_+^{(1)} \exp(\mathrm{i}k_{z\phi}^{(1)} z) + \sum_{q=1}^{Q} a_-^{(q)} \phi^{(q)} \exp(-\mathrm{i}k_{z\phi}^{(q)} z), \quad \text{inlet,} \tag{30}$$

$$\Psi_4 = \sum_{q=1}^{Q} c_+^{(q)} \phi^{(q)} \exp(\mathrm{i}k_{z\phi}^{q}(z-\ell)) + c_-^{(1)} \exp(-\mathrm{i}k_{z\phi}^{(1)}(z-\ell)), \quad \text{outlet,} \tag{31}$$

where $\phi^{(q)}(r, \varphi)$ is normalized to give $\phi^{(1)} = 1$. The eigenmodes of the homogenous and non-dissipative inlet/outlet can be shown to form a complete set and it is also possible, and quite straightforward, to formulate an orthogonality relation [11],

$$\int_{S_1} \phi^{(q)} \phi^{(u)} \, \mathrm{d}S = \begin{cases} \Lambda_\phi^{(u)} & \text{for } q = u, \\ 0 & \text{else,} \end{cases} \tag{32}$$

which subsequently will prove useful. For the non-homogenous dissipative duct, the situation is somewhat more complicated. For this part, the eigenvalue problem is not real-valued and there is, to the author's knowledge, no proof available in the literature as to whether a set of eigenmodes is complete or not in the case of complex eigenvalues. One may, however, argue that if the set is complete in the corresponding real case, it is, by analytical continuation, also complete in the complex case. Even though a true orthogonality relation does not exist it is still possible to formulate a similar and equally useful relation also for the eigenmodes of the dissipative duct (see, for instance, reference [12]),

$$\int_{S_1} \rho_1 \psi_1^{(s)} \psi_1^{(v)} \, \mathrm{d}S + \int_{S_2} \rho_2 \psi_2^{(s)} \psi_2^{(v)} \, \mathrm{d}S = \begin{cases} \Lambda_\Psi^{(v)} & \text{for } s = v, \\ 0 & \text{else,} \end{cases} \tag{33}$$

By utilization of the longitudinal boundary and coupling conditions, the following relations involving the unknown coefficients $a_+^{(1)}, a_-^{(1)}, a_-^{(2)}, \ldots, c_+^{(Q)}$ can be formulated for $z = 0$,

$$a_{+1}^{(1)} + \sum_{q=1}^{Q} a_-^{(q)} \phi^{(q)} = \sum_{s=1}^{S} \psi_1^{(s)} (b_+^{(s)} + b_-^{(s)} \exp(\mathrm{i} k_{z\Psi}^{(s)} \ell)), \quad (r, \varphi) \in S_1, \tag{34}$$

$$\mathrm{i} k_{z\phi}^{(1)} a_+^{(1)} - \sum_{q=1}^{Q} \mathrm{i} k_{z\phi}^{(1)} a_-^{(q)} \phi^{(q)} = \sum_{s=1}^{S} \mathrm{i} k_{s\Psi}^{(s)} \psi_1^{(s)} (b_+^{(s)} - b_-^{(s)} \exp(\mathrm{i} k_{z\Psi}^{(s)} \ell)), \quad (r, \varphi) \in S_1, \tag{35}$$

$$\sum_{s=1}^{S} \mathrm{i} k_{s\Psi}^{(s)} \psi_2^{(s)} (b_+^{(s)} - b_-^{(s)} \exp(\mathrm{i} k_{z\Psi}^{(s)} \ell)) = 0, \quad (r, \varphi) \in S_2, \tag{36}$$

and for $z = l$,

$$c_-^{(1)} + \sum_{q=1}^{Q} c_+^{(q)} \phi^{(q)} = \sum_{s=1}^{S} \psi_1^{(s)} (b_+^{(s)} \exp(\mathrm{i} k_{z\Psi}^{(s)} \ell) + b_-^{(s)}), \quad (r, \varphi) \in S_1, \tag{37}$$

$$\sum_{q=1}^{Q} \mathrm{i} k_{z\phi}^{(q)} c_+^{(q)} \phi^{(q)} - \mathrm{i} k_{z\phi}^{(1)} c_-^{(1)} = \sum_{s=1}^{S} \mathrm{i} k_{z\Psi}^{(s)} \psi_1^{(s)} (b_+^{(s)} \exp(\mathrm{i} k_{z\Psi}^{(s)} \ell) - b_-^{(s)}), \quad (r, \varphi) \in S_1, \tag{38}$$

$$\sum_{s=1}^{S} \mathrm{i} k_{s\Psi}^{(s)} \psi_2^{(s)} (b_+^{(s)} \exp(\mathrm{i} k_{z\Psi}^{(s)} \ell) - b_-^{(s)}) = 0, \quad (r, \varphi) \in S_2 \tag{39}$$

respectively. It is possible to obtain the coefficients from these relations directly by yet again employing collocation as suggested by Munjal [13]. Here, however, as the inlet and outlet boundaries of the lined duct are quite irregular, more accurate results are obtained if the polar dependence of the eigenmodes is eliminated by integration over the corresponding

cross-section, thus replacing the requirements on pointwise fulfilment of the boundary and coupling conditions by equality in mean. To obtain a well-defined system of equations, eqs (34)–(39) must, preceding the integration, be multiplied by a number of linearly indepedent weighting functions. In this procedure it may be suitable to identify these functions as the given eigenmodes and thus utilize the relations (32) and (33). This technique to produce a weak formulation of the problem is traditionally termed mode-matching. Thus, by multiplication of the pressure relations (34) and (37) with $\phi^{(u)}$, $u = 1, \ldots, Q$, and then integration over S_1, equation (34) gives

$$S_1(a_+^{(1)} + a_-^{(1)}) = \sum_{s=1}^{S} [b_+^{(s)} + b_-^{(s)} \exp(\mathrm{i}k_{z\Psi}^{(s)}\ell)] \int_{S_1} \psi_1^{(s)} \, \mathrm{d}S, \tag{40}$$

$$\Lambda_\phi^{(u)} a_-^{(u)} = \sum_{s=1}^{S} [b_+^{(s)} + b_-^{(s)} \exp(\mathrm{i}k_{z\Psi}^{(s)}\ell)] \int_{S_1} \phi^{(u)} \psi_1^{(s)} \, \mathrm{d}S, \quad u = 2, 3, \ldots, Q, \tag{41}$$

$$S_1(c_+^{(1)} + c_-^{(1)}) = \sum_{s=1}^{S} [b_+^{(s)} \exp(\mathrm{i}k_{z\Psi}^{(s)}\ell) + b_-^{(s)}] \int_{S_1} \psi_1^{(s)} \, \mathrm{d}S, \tag{42}$$

$$\Lambda_\phi^{(u)} c_-^{(u)} = \sum_{s=1}^{S} [b_+^{(s)} \exp(\mathrm{i}k_{z\Psi}^{(s)}\ell) + b_-^{(s)}] \int_{S_1} \phi^{(u)} \psi_1^{(s)} \, \mathrm{d}S, \quad u = 2, 3, \ldots, Q. \tag{43}$$

Similarly, the "orthogonality relation" for the dissipative duct (33) can be utilized by first multiplying the velocity continuity condition (35) with $\rho_1 \psi_1^{(v)}$ and integrating over S_1, then multiplying the boundary condition (36) with $\rho_2 \psi_2^{(v)}$ and integrating over S_2 and finally adding the obtained expressions:

$$\begin{aligned} &\rho_1 k_{z\phi}^{(1)} (a_+^{(1)} - a_-^{(1)}) \int_{S_1} \psi_1^{(v)} \, \mathrm{d}S - \sum_{q=2}^{Q} \rho_1 k_{z\phi}^{(q)} a_-^{(q)} \int_{S_1} \phi^{(q)} \psi_1^{(v)} \, \mathrm{d}S \\ &\quad = k_{z\Psi}^{(v)} \Lambda_\Psi^{(v)} [b_+^{(v)} - b_-^{(v)} \exp(\mathrm{i}k_{z\Psi}^{(v)}\ell)], \quad v = 1, \ldots, S. \end{aligned} \tag{44}$$

Eventually, in the case of negligible dissipation and solely plane waves these relations are reduced to the classical requirement on continuity in acoustic volume flow across the area change. The same procedure can also be performed at $z = \ell$ for conditions (38) and (39) giving

$$\begin{aligned} &\rho_1 k_{z\phi}^{(1)} (c_+^{(1)} - c_-^{(1)}) \int_{S_1} \psi_1^{(v)} \, \mathrm{d}S + \sum_{q=2}^{Q} \rho_1 k_{z\phi}^{(q)} c_+^{(q)} \int_{S_1} \phi^{(q)} \psi_1^{(v)} \, \mathrm{d}S \\ &\quad = k_{z\Psi}^{(v)} \Lambda_\Psi^{(v)} [b_+^{(v)} \exp(\mathrm{i}k_{z\Psi}^{(v)}\ell) - b_-^{(v)}], \quad v = 1, \ldots, S. \end{aligned} \tag{45}$$

Equations (40)–(45) constitute a system of $2Q + 2S$ linear equations for, as the incident plane wave is known either at the inlet or at the outlet, an equal number of unknowns. Usually, it is numerically suitable to try to derive closed-form expressions for some of the unknowns and thus enable compression of the system before solving it. This can be done in a number of ways and in most cases the best formulation is decided upon by the size and the

range of the different parameters, e.g. frequency or attenuation. One alternative is to solve the expansion coefficients for the dissipative duct from equations (44) and (45),

$$b_+^{(v)} = \frac{\rho_1}{k_{z\Psi}^{(v)} \Lambda_\Psi^{(v)} [1 - \exp(2\mathrm{i} k_{z\Psi}^{(v)} \ell)]} \left\{ k_{z\phi}^{(1)} \int_{S_1} \psi_1^{(v)} \, \mathrm{d}S [a_+^{(1)} - a_-^{(1)} - (c_+^{(1)} - c_-^{(1)}) \exp(\mathrm{i} k_{z\Psi}^{(v)} \ell)] \right.$$
$$\left. - \sum_{q=2}^{Q} k_{z\phi}^{(q)} \int_{S_1} \phi^{(q)} \psi_1^{(v)} \, \mathrm{d}S [a_-^{(q)} + \exp(\mathrm{i} k_{z\Psi}^{(v)} \ell) c_+^{(q)}] \right\}, \quad v = 1, \ldots, S, \tag{46}$$

$$b_-^{(v)} = \frac{\rho_1}{k_{z\Psi}^{(v)} \Lambda_\Psi^{(v)} [1 - \exp(2\mathrm{i} k_{z\Psi}^{(v)} \ell)]} \left\{ k_{z\phi}^{(1)} \int_{S_1} \psi_1^{(v)} \, \mathrm{d}S [(a_+^{(1)} - a_-^{(1)}) \exp(\mathrm{i} k_{z\Psi}^{(v)} \ell) - c_+^{(1)} + c_-^{(1)}] \right.$$
$$\left. - \sum_{q=2}^{Q} k_{z\phi}^{(q)} \int_{S_1} \phi^{(q)} \psi_1^{(v)} \, \mathrm{d}S [a_-^{(q)} \exp(\mathrm{i} k_{z\Psi}^{(v)} \ell) + c_+^{(q)}] \right\}, \quad v = 1, \ldots, S. \tag{47}$$

By inserting these expressions into the system given by equations (40)–(43) and defining the state variables usually associated with the acoustic transfer matrix, i.e., plane wave pressure and volume velocity at the inlet and outlet sections,

$$p_1 = -\mathrm{i}\omega\rho_1 (a_+^{(1)} + a_-^{(1)}), \tag{48}$$

$$U_1 = -\mathrm{i} k_{z\phi}^{(1)} S_1 (a_+^{(1)} - a_-^{(1)}), \tag{49}$$

$$p_2 = -\mathrm{i}\omega\rho_1 (c_+^{(1)} + c^{(1)}), \tag{50}$$

$$U_2 = -\mathrm{i} k_{z\phi}^{(1)} S_1 (c_+^{(1)} - c_-^{(1)}), \tag{51}$$

among which the variables on the outlet/downstream side are assumed to be known, a system of linear equations for $2Q$ unknowns; p_1, U_1 along with $a^{(2)}, \ldots, a^{(Q)}$ and $c_1^{(2)}, \ldots, c_1^{(Q)}$ is obtained:

$$-S_1^2 p_1 + \rho_1 c_1 \mathrm{K}_b^{(1,1)} U_1 + \sum_{q=2}^{Q} \mathrm{i}\omega\rho_1 S_1 (\mathrm{K}_b^{(1,q)} a_-^{(q)} + \mathrm{K}_a^{(1,q)} c_+^{(q)}) = \rho_1 c_1 \mathrm{K}_a^{(1,1)} U_2, \tag{52}$$

$$\rho_1 c_1 \mathrm{K}_a^{(1,1)} U_1 + \sum_{q=2}^{Q} \mathrm{i}\omega\rho_1 S_1 (\mathrm{K}_a^{(1,q)} a_-^{(q)} + \mathrm{K}_b^{(1,q)} c_+^{(q)}) = S_1^2 p_2 + \rho_1 c_1 \mathrm{K}_b^{(1,1)} U_2, \tag{53}$$

$$c_1 \mathrm{K}_b^{(p,1)} U_1 + \mathrm{i}\omega S_1 \sum_{q=2}^{Q} [(\mathrm{K}_b^{(p,q)} + \Lambda_\phi^{(p)} \delta_{pq}) a_-^{(q)} + \mathrm{K}_a^{(p,q)} c_+^{(q)}] = c_1 \mathrm{K}_a^{(p,1)} U_2, \quad p = 2, 3, \ldots, Q, \tag{54}$$

$$c_1 \mathrm{K}_a^{(p,1)} U_1 + \mathrm{i}\omega S_1 \sum_{q=2}^{Q} [\mathrm{K}_a^{(p,q)} a_-^{(q)} + (\mathrm{K}_b^{(p,q)} + \Lambda_\phi^{(p)} \delta_{pq}) c_+^{(q)}] = c_1 \mathrm{K}_b^{(p,1)} U_2, \quad p = 2, 3, \ldots, Q, \tag{55}$$

where δ_{pq} is the Kronecker delta and

$$\left.\begin{matrix} K_a^{(p,q)} \\ K_b^{(p,q)} \end{matrix}\right\} = \sum_{s=1}^{S} \frac{\mathrm{i}k_{z\phi}^{p}\rho_1}{k_{z\Psi}^{(s)}\Lambda_{\Psi}^{(s)}\sin(k_{z\Psi}^{(s)}\ell)} \int_{S_1} \phi^{(p)}\psi_1^{(s)}\,\mathrm{d}S \int_{S_1} \phi^{(q)}\psi_1^{(s)}\,\mathrm{d}S \left\{\begin{matrix} 1 \\ \cos(k_{z\Psi}^{(s)}\ell) \end{matrix}\right. . \tag{56}$$

In matrix form, this system reads

$$\mathbf{A}\mathbf{x} = \mathbf{b}, \tag{57}$$

where $\mathbf{A}$ apparently has the dimension $2Q \times 2Q$ and the elements given by equations (52)–(55). The unknowns are arranged as

$$\mathbf{x}^{\mathrm{T}} = (p_1, U_1, a_-^{(2)}, c_+^{(2)}, \ldots, a_-^{(Q)}, c_+^{(Q)}), \tag{58}$$

whereas the right-hand side reads

$$\begin{aligned} \mathbf{b}^{\mathrm{T}} = (&\rho_1 c_1 K_a^{(1,1)} U_2,\ S_1^2 p_2 + \rho_1 c_1 K_b^{(1,1)} U_2,\ c_1 K_a^{(2,1)} U_2,\ c_1 K_b^{(2,1)} U_2, \\ &\ldots, c_1 K_a^{(Q,1)} U_2,\ c_1 K_b^{(Q,1)} U_2). \end{aligned} \tag{59}$$

It may be noted that for a silencer with very poor dissipation, the longitudinal wavenumber of the dissipative duct, $k_{z\Psi}^{(s)}$, might become almost real and thus whenever there is a longitudinal resonance in the silencer, the constants specified in equation (56) tends towards infinity and thus $\mathbf{A}$ becomes numerically ill-conditioned. This is in most cases somewhat academic as the typical dissipative silencer has quite a large rate of dissipation. However, if the formulation is required to handle the reactive case as well, it might be suitable, by use of equations (41) and (43) to eliminate the inlet and outlet expansion coefficients and obtain instead a $(2S + 2) \times (2S + 2)$ matrix to solve for the dissipative field and the inlet plane wave. As the number of modes required in each part to obtain a certain accuracy is related to the dimensions of the cross-section and thus $S > Q$, this latter system is numerically larger even though, for some symmetrical cases, the matrix is sparse.

It might in this context be appropriate to mention briefly the matter of relative convergence associated with the mode-matching technique. As the partial field expansions (28)–(31) are truncated in the above derivation and the system (57) is well-defined no matter how this is performed "in detail", the question arises as to whether the relation between the number of modes included in each region is optional or not. For lower and moderate number of modes, different ratios S/Q would be expected to give different solutions. On the other hand, when the number of modes in the different regions tends towards infinity, one might expect the result to be independent of this ratio. As shown by Mittra [14] when analyzing the similar problem of mode matching in a 2-D bifurcated duct, this is however not always the case and accordingly false solutions may be obtained. By use of the edge condition, Mittra was able to derive a simple and very useful relationship between the mode ratio and the cross-sectional dimensions that warrants an unique solution and thus prevents relative convergence in the case of the bifurcated duct. Even though the sudden expansion/contraction encountered in this problem also possesses a geometrical singularity with an appending edge condition and thus perhaps would be expected to need a similar relationship, there are some numerical investigations [15, 16], performed for the

corresponding 2-D problem, that indicates this not to be the case. Nevertheless, there may still be an optimum mode ratio which will give the fastest numerical convergence. In the 2-D axisymmetric circular-circular case, this reads $S/Q \approx b/a$ which eventually, as discussed by Leroy [17], is also the choice that may be concluded from the work of Mittra. In addition, this choice has also been put forward by Hudde *et al.* [18] by reasoning in terms of the modal amplitudes in the different regions. In the 3-D case, it seems, as suggested by Vassallo [15], reasonable to assume the relation to be $S/Q \approx S_2/S_1$, i.e., proportional to the ratio of the modal densities at each side of the expansion/contraction.

Finally, to obtain the transfer matrix elements, $t_{11}, \ldots, t_{22}$, defined from

$$\begin{bmatrix} p_1 \\ U_1 \end{bmatrix} = \begin{bmatrix} t_{11} & t_{12} \\ t_{21} & t_{22} \end{bmatrix} \begin{bmatrix} p_2 \\ U_2 \end{bmatrix}, \tag{60}$$

the "two-load technique" proposed by Åbom [19] is well suited. By this approach the silencer is first analyzed with the outlet "closed", $U_2 = 0$. By also specifying $p_2 = 1$, this corresponds to a right-hand side of equation (57) as $\mathbf{b}^{\mathrm{T}} = (0, S_1^2, 0, \ldots, 0)$ and gives the upper row of the transfer matrix as the first two components of $\mathbf{x}$, i.e., $t_{11} = x_1|_{\text{load 1}}$ and $t_{21} = x_2|_{\text{load 1}}$. The outlet is then shifted to "pressure release", $p_2 = 0$ which with $U_2 = 1$ in turn corresponds to a right-hand side as

$$\mathbf{b}^{\mathrm{T}} = (\rho_1 c_1 K_a^{(1,1)}, \rho_1 c_1 K_b^{(1,1)}, c_1 K_a^{(2,1)}, c_1 K_b^{(2,1)}, \ldots, c_1 K_a^{(Q,1)}, c_1 K_b^{(Q,1)}). \tag{61}$$

and in the same way gives the two remaining parameters, $t_{12} = x_1|_{\text{load 2}}$ and $t_{22} = x_2|_{\text{load 2}}$. The transfer matrix for the dissipative silencer may consequently be written as

$$\begin{bmatrix} p_1 \\ U_1 \end{bmatrix} = \begin{bmatrix} x_1|_{\text{load 1}} & x_1|_{\text{load 2}} \\ x_2|_{\text{load 1}} & x_2|_{\text{load 2}} \end{bmatrix} \begin{bmatrix} p_2 \\ U_2 \end{bmatrix}. \tag{62}$$

4. NUMERICAL RESULTS

The formulation given above has been implemented on a PC-Pentium, 100 MHz using Standard FORTRAN with double precision running under MS-DOS. This somewhat unsophisticated choice of computational environment is motivated by the most important question of engineering applicability set upon most numerical simulation codes. It also means that all numerical simulations are handled within a primary memory capacity of 640 kb. It should be noted at this point that all results presented below are achieved within a typical CPU-time of a couple of minutes.

To ensure that the dispersion relation (26) is correctly solved and that no eigenvalues are lost or mixed, a dedicated scheme has been developed. First, for a given frequency, the amount of dissipation is reduced to a minimum to gather the transverse wavenumbers along the real axis in the complex $k_{\perp 1}$ plane. To isolate and locate the roots approximately, the principle of arguments is then applied [20]. This will also reveal any possible degeneracy of the eigenvalues. The approximate locations of the eigenvalues are then used to initiate a secant search to the desired accuracy. Once a root has been accurately determined, the rate of dissipation is stepwise increased to its actual value and the root being traced throughout this process, again using the secant method. In this material stepping the initial values for the current material point are linearly extrapolated from the results of the two

preceding points. This technique is clearly not applicable until the first two points have been analyzed and therefore the second point in some cases is just a slight perturbation of the starting point. To increase the speed of the material stepping in a such an application, a gradually increase in stepsize, reflecting the asymptotic behaviour of the problem, is used. A similar tracing of the roots is used also for the frequency stepping. Due to the simplicity of the collocation method the speed of the briefed eigenvalue solver is high and the number of frequency points may well be of the order 10^3 which is sufficient for most applications. The corresponding eigenmodes are obtained by solving equation (25) using inverse iteration [21].

The mode matching, which in this context may be termed numerical to highlight the fact that the eigenmodes are numerically determined, requires a number of integrals within equations (52)–(56) involving products of Bessel functions, to be calculated. With the chosen restriction to a circular central passage and inlet/outlet, the CPU time may be reduced using analytical expressions [22] for some of the integrals. Thus,

$$\Lambda_{\phi}^{(u)} = \frac{\pi a^2}{2}\left[1 - (n/k_r^{(u)}a)^2\right] \mathrm{J}_n^2(k_r^{(u)}a) \tag{63}$$

and

$$\begin{aligned}
\Lambda_{\Psi}^{(v)} = {} & \rho_1 \frac{\pi}{2} \sum_{n=0}^{N} (1+\delta_{0n})[(A_n^{(v)})^2 + (B_n^{(v)})^2]\left\{\mathrm{J}_n'^2(k_{\perp 1}^{(v)}a) + \left[1 - (n/k_{11}^{(v)}a)^2\right]\mathrm{J}_n^2(k_{\perp 1}^{(v)}a)\right\} \\
& + \rho_2 \sum_{n=0}^{M}\sum_{m=0}^{M}\left[C_n^{(v)}C_m^{(v)}\int_0^{2\pi}\int_a^{b(\varphi)} \mathrm{J}_n(k_{\perp 2}^{(v)}r)\mathrm{J}_m(k_{\perp 2}^{(v)}r)\cos n\varphi\cos m\varphi r\,\mathrm{d}\,\mathrm{d}\varphi\right. \\
& + D_n^{(v)}D_m^{(v)}\int_0^{2\pi}\int_a^{b(\varphi)} \mathrm{J}_n(k_{\perp 2}^{(v)}r)\mathrm{J}_m(k_{\perp 2}^{(v)}r)\sin n\varphi\sin m\varphi r\,\mathrm{d}r\,\mathrm{d}\varphi \\
& + E_n^{(v)}E_m^{(v)}\int_0^{2\pi}\int_a^{b(\varphi)} \mathrm{N}_n(k_{\perp 2}^{(v)}r)\mathrm{N}_m(k_{\perp 2}^{(v)}r)\cos n\varphi\cos m\varphi r\,\mathrm{d}r\,\mathrm{d}\varphi \\
& + F_n^{(v)}F_m^{(v)}\int_0^{2\pi}\int_a^{b(\varphi)} \mathrm{N}_n(k_{\perp 2}^{(v)}r)\mathrm{N}_m(k_{\perp 2}^{(v)}r)\sin n\varphi\sin m\varphi r\,\mathrm{d}r\,\mathrm{d}\varphi \\
& + 2C_n^{(v)}D_m^{(v)}\int_0^{2\pi}\int_a^{b(\varphi)} \mathrm{J}_n(k_{\perp 2}^{(v)}r)\mathrm{J}_m(k_{\perp 2}^{(v)}r)\cos n\varphi\sin m\varphi r\,\mathrm{d}r\,\mathrm{d}\varphi \\
& + 2C_n^{(v)}E_m^{(v)}\int_0^{2\pi}\int_a^{b(\varphi)} \mathrm{J}_n(k_{\perp 2}^{(v)}r)\mathrm{N}_m(k_{\perp 2}^{(v)}r)\cos n\varphi\cos m\varphi r\,\mathrm{d}r\,\mathrm{d}\varphi \\
& + 2C_n^{(v)}F_m^{(v)}\int_0^{2\pi}\int_a^{b(\varphi)} \mathrm{J}_n(k_{\perp 2}^{(v)}r)\mathrm{N}_m(k_{\perp 2}^{(v)}r)\cos n\varphi\sin m\varphi r\,\mathrm{d}r\,\mathrm{d}\varphi \\
& + 2D_n^{(v)}E_m^{(v)}\int_0^{2\pi}\int_a^{b(\varphi)} \mathrm{J}_n(k_{\perp 2}^{(v)}r)\mathrm{N}_m(k_{\perp 2}^{(v)}r)\sin n\varphi\cos m\varphi r\,\mathrm{d}r\,\mathrm{d}\varphi \\
& + 2D_n^{(v)}F_m^{(v)}\int_0^{2\pi}\int_a^{b(\varphi)} \mathrm{J}_n(k_{\perp 2}^{(v)}r)\mathrm{N}_m(k_{\perp 2}^{(v)}r)\sin n\varphi\sin m\varphi r\,\mathrm{d}r\,\mathrm{d}\varphi \\
& \left. + 2E_n^{(v)}F_m^{(v)}\int_0^{2\pi}\int_a^{b(\varphi)} \mathrm{N}_n(k_{\perp 2}^{(v)}r)\mathrm{N}_m(k_{\perp 2}^{(v)}r)\cos n\varphi\sin m\varphi r\,\mathrm{d}r\,\mathrm{d}\varphi\right]
\end{aligned} \tag{64}$$

as well as

$$\int_{S_1} \phi^{(p)} \psi_1^{(s)} \, \mathrm{d}S = \pi(1 + \delta_{0n}) \frac{k_r^{(p)} a \mathrm{J}_n(k_{\perp 1}^{(s)} a) \mathrm{J}_n'(k_r^{(p)} a) - k_{\perp 1}^{(s)} a \mathrm{J}_n(k_r^{(p)} a) \mathrm{J}_n'(k_{\perp 1}^{(s)} a)}{(k_{\perp 1}^{(s)})^2 - (k_r^{(p)})^2}$$

$$\begin{cases} A_n^{(s)} \cos n\varphi \\ B_n^{(s)} \sin n\varphi \end{cases} \tag{65}$$

the last integral being part of expression (56). What remains to be calculated is apparently the integrals within equation (64). To cope with, this Romberg's method [21], i.e., the trapezoidal rule with repeated Richardson extrapolation, is applied.

The whole numerical code is run within the framework of SID [23] which is an engineering tool for design and analysis of flow ducts based on the acoustic two-port method and by which the interaction between the dissipative silencer and other silencers in, for example, an automotive exhaust system, may be analyzed.

4.1. AN ELLIPTIC DISSIPATIVE SILENCER

In order to test in some way the formulation suggested above, the transmission loss of a dissipative silencer with an elliptic cross-section has been calculated for a selection of geometrical and material data representative of a typical automotive exhaust silencer and readily available. Obviously, the given formulation may also be applied to other kinds of bulk-reacting lined ducts such as, e.g. ventilation silencers, provided of course that the fundamental assumptions stated above in section 2 holds.

Often the dissipative automotive silencer has an eccentric in/outlet, in most cases due to lack of space beneath the car, but the question may arise as to whether this may have any significant influence upon the acoustic transmission properties or not. For an elliptic cross-section with the origin located at (x_0, y_0), Γ_2 is given by

$$b = [x_0 b_{min}^2 \cos\varphi + y_0 b_{max}^2 \sin\varphi + b_{min} b_{max} \sqrt{b_{min}^2 \cos^2\varphi + b_{max}^2 \sin^2\varphi - (y_0 \cos\varphi - x_0 \sin\varphi)^2}]/ \\ (b_{min}^2 \cos^2\varphi + b_{max}^2 \sin^2\varphi). \tag{66}$$

In the following example, $b_{min}/b_{max} = \sqrt{0{\cdot}51}$, which corresponds to an eccentricity of 0·7. To normalize the results, the radius of the area equivalent circle, $b_m = \sqrt{b_{min} b_{max}}$, will be used. The radius of the circular central passage is chosen to be $0{\cdot}4193 b_m$ and the length of the silencer is set to $4b_m$.

The porous material is described by the Delany and Bazley formulae [24],

$$c_2 = \frac{c_1}{(1 + \alpha_7 \eta^{\alpha_8} - \mathrm{i}\alpha_5 \eta^{\alpha_6})} \tag{67}$$

$$\rho_2 = \rho_1 (1 + \alpha_1 \eta^{\alpha_2} - \mathrm{i}\alpha_3 \eta^{\alpha_4})(1 + \alpha_7 \eta^{\alpha_8} - \mathrm{i}\alpha_5 \eta^{\alpha_6}), \tag{68}$$

where $\eta = k_1 b_m / 2\pi \Phi_n$, in which $\Phi_n = \Phi b_m / \rho_1 c_1$ is the normalized flow resistance. The coefficients are chosen from measurements upon basalt wool made by Cummings [25]; $\alpha_1 = 0{\cdot}0414$, $\alpha_2 = -0{\cdot}0774$, $\alpha_3 = 0{\cdot}124$, $\alpha_4 = -0{\cdot}645$, $\alpha_5 = 0{\cdot}196$, $\alpha_6 = -0{\cdot}639$, $\alpha_7 = 0{\cdot}0971$ and $\alpha_8 = -0{\cdot}749$.

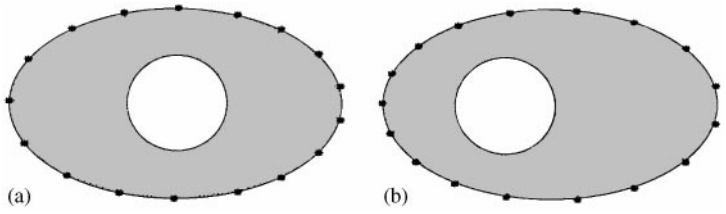

Figure 2. The collocation grids for the two cross-sections analyzed.

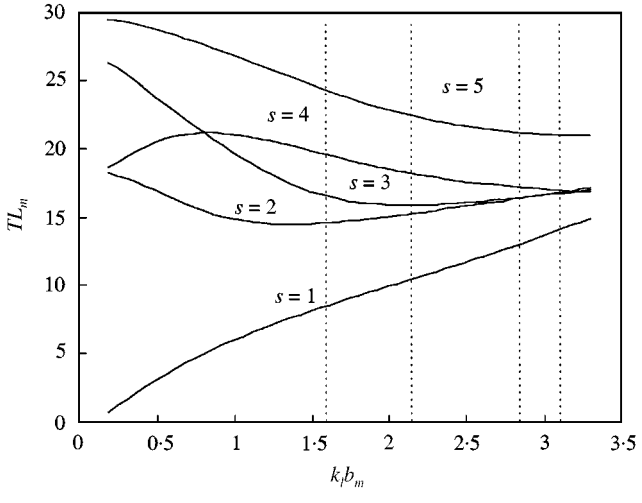

Figure 3. The transmission loss per length of the five lowest eigenmodes with a *concentric* central passage as shown in Figure 2(a). The dotted lines represents the cut-on values of the higher order modes in the corresponding non-dissipative duct.

To address the question posed above, a concentric as well as an eccentric in/outlet, $x_0 = 0{\cdot}3b_m$, is analyzed for $\Phi_n = 2{\cdot}91$. A moderate number of terms are chosen in the expansions of the eigenmodes, $M = 8$, i.e., 17 points are used for the collocation. The points are chosen with slight decrease in polar angle step at the vicinity of the major axis; see Figure 2 above. With these collocation grids, the accuracy of the obtained eigenvalues are to at least 4 figures. The eigenvalues corresponding to the 5 lowest modes of the lined duct have been traced for the Helmholtz number, kb_m from 0·2 to 3·3 using 2001 equidistant points, and from 0·2 to 18·3 using 300 points and gradually increasing stepsize, for the concentric and eccentric case respectively. The latter frequency range, corresponding to the full range of validity for the Delany and Bazley model, greatly exceeds the range of practical interest for commercial dissipative silencers but is included merely to illustrate the possibility of analyzing higher Helmholtz numbers with given formulation. In Figures 3 and 4 the results are presented in terms of transmission loss per length b_m, $TL_m = 20\,|\mathrm{Im}(k_{z\Psi} b_m)|\log_{10}(e)$. It can be seen from these figures, especially Figure 4, that the eigenmodes asymptotically tend towards the same attenuation. This would imply that no matter which eigenmode is most strongly excited in a practical installation of a dissipative silencer, the attenuation will still be the same for the higher frequencies.

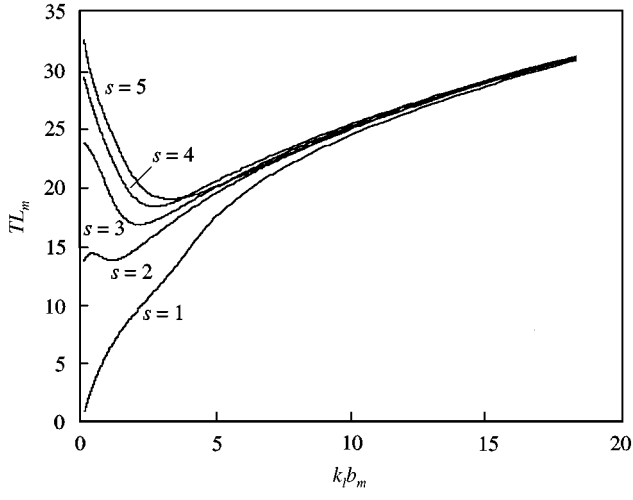

Figure 4. The transmission loss per length of the five lowest modes with an *eccentric* central passage, $x_0 = 0{\cdot}3b_m$, as shown in Figure 2(b).

From the elements of the transfer matrix (60) the overall transmission loss of the dissipative silencer may be calculated from

$$TL = 10\log_{10}|t_{11} + t_{12}S_1/\rho_1 c_1 + t_{21}\rho_1 c_1/S_1 + t_{22}|, \tag{69}$$

which in order to enable comparison with earlier results will also be expressed in terms of attenuation per length b_m. The result calculated for the concentric as well as the eccentric case using 51 points is shown in Figure 5. In the lined duct, all the eigenmodes analyzed above are included in the mode matching; $Q = 5$, whereas within the inlet and outlet sections only the fundamental mode is considered; $S = 1$. This choice is, of course, optional but could be motivated by restricting the analysis to modes that are cut-on in the corresponding non-attenuated case. The remaining higher order modes will typically also be too attenuated to give any significant effect in a silencer of the given length to width ratio. The chosen number of modes also agrees with the optimum modal ratio suggested above. As seen in Figure 5 the concentric configuration gives the largest attenuation except at the lowest frequencies where the predominating fundamental mode is almost plane and consequently the cross-sectional shape is less important.

A technique often used in the analysis of dissipative silencers is to restrict the analysis to only the fundamental modes, not only in the in/outlet but also in the lined duct. In Figures 6 and 7, the transmission loss obtained by this technique is compared to the more accurate mode-matching results presented above but also with the transmission loss of the fundamental mode itself. Apparently, from an engineering point of view, both the estimate based on the attenuation per length of the fundamental mode as well as on the "plane wave" analysis gives acceptable results although as expected with a slight, typically 1–2 dB, underestimate of the attenuation. It must be remembered though that this is not a general result; with a less resistive porous material a different result would be obtained. This is illustrated in Figure 8 where the same eccentric configuration has been analyzed, though now with the flow resistivity reduced to one-third; $\Phi_n = 0{\cdot}97$. The attenuation is now underestimated by the fundamental mode solution by around 20% but perhaps more

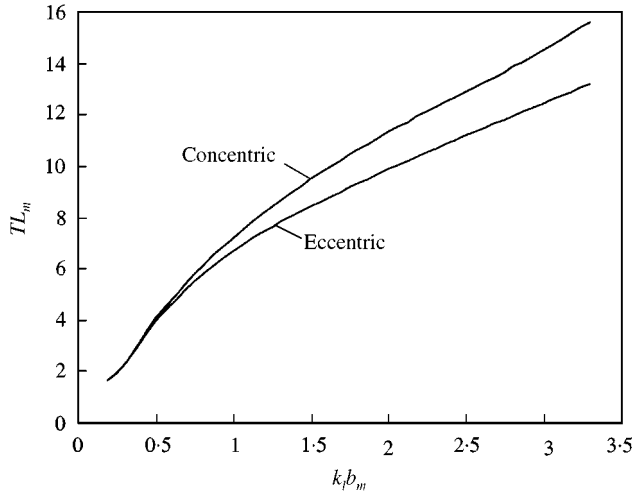

Figure 5. Comparison between the transmission loss per length for a silencer with concentric, and eccentric, $x_0 = 0{\cdot}3b_m$, in/outlet.

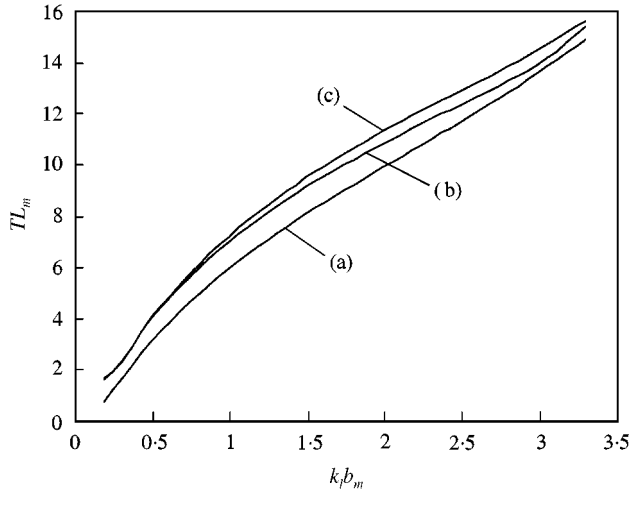

Figure 6. The transmission loss per length for a *concentric* dissipative silencer estimated by; (a) attenuation of fundamental mode per length, (b) mode matching by using solely fundamental modes, and (c) mode matching using the five lowest modes of the lined duct.

interesting is the slight *overestimate* of the attenuation at higher frequencies obtained by the plane wave solution. Clearly, this effect is due to the onset of higher order modes which in this less dissipative case is more pronounced.

Even though it is clear from the results above that efficient optimization of the dissipative silencer requires detailed modelling of the acoustic field, it is also apparent that not only the plane wave but also the fundamental mode estimate may be of use in many practical applications, especially as the parameter values chosen in these simulations are realistic values obtained from measurements on commercial silencers.

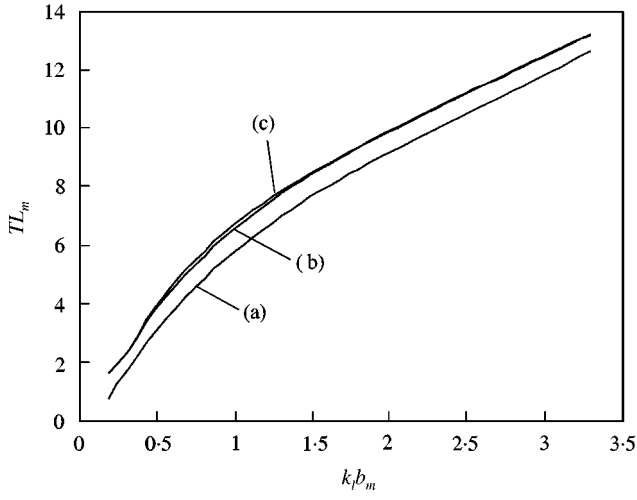

Figure 7. The transmission loss per length of an *eccentric* dissipative silencer estimated by (a) attenuation of fundamental mode per length, (b) mode matching using solely fundamental modes, and (c) mode matching using the five lowest modes of the lined duct.

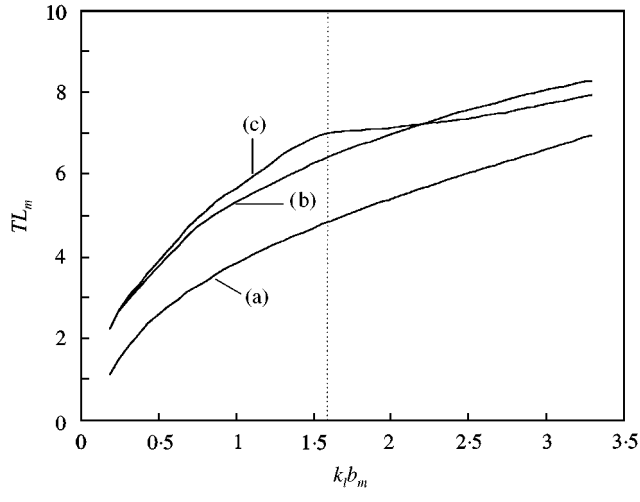

Figure 8. The transmission loss per length of an *eccentric* dissipative silencer with reduced flow resistivity; $\Phi_n = 0{\cdot}97$, estimated by (a) attenuation of fundamental mode per length, (b) mode matching using solely fundamental modes, and (c) mode matching using the five lowest modes of the lined duct. The dotted line represents the cut-on of the first higher order mode.

5. CONCLUSIONS

The transfer matrix for a cylindrical dissipative silencer of arbitrary cross-section and inlet/outlet has been derived for the case of negligible mean flow. Unlike most earlier contributions in literature, which are restricted to axisymmetric configurations, this analysis is completely 3-D including also the outer end corrections, i.e., the near field in the

inlet/outlet ducts. The derivation is based on a two-step procedure first using collocation to determine the wavenumbers and eigenmodes of the lined duct section and, secondly, coupling the partial fields of the inlet, outlet and lined duct respectively by mode matching. As an expansion in the polar eigenfunctions is used for the modal amplitudes, the formulation gives optimum convergence for circular-like geometries and a residual confined to the boundary conditions. The mode-matching scheme utilizes orthogonality, or orthogonality-like, properties of the eigenmodes in *both* the inlet/outlet and the dissipative duct. By this approach, the system to be solved for the transfer matrix elements can be reduced to give a numerically smaller problem than that obtained in the more common one-sided approach. By restricting the analysis to configurations with circular in/outlet and a central passage, the numerical problem may be further reduced by performing collocation solely at the outer boundary and solving some of the mode-matching integrals analytically. In order to emphasize the fact that in this problem there are geometrical singularities, a brief discussion about the closely related matter of relative convergence is given, although no problems are likely to arise here.

As a practical application, a dissipative automotive silencer of elliptic cross-section has been analyzed briefly regarding the in/outlet location and rate of dissipation. In this analysis, the full mode-matching formulation has been compared to both a fundamental mode estimate as well as a "plane wave" model. The results obtained for typical, but not too low, values of flow resistivity show reasonable agreement between the three different estimates, which consequently implies that for certain applications the most simple fundamental mode estimate may well suffice. On the other hand, for applications with lower rates of dissipation, or higher demands for accurate optimization, a more detailed but still numerically manageable analysis such as the suggested formulation is needed.

A major advantage with this technique compared to, for example conventional FEM, is the close resemblance to the case of a circular cylindric expansion chamber. By this the management and interpretation of the results are made much easier. Another useful feature enabled by the numerical efficiency is the possibility of starting the analysis at a known configuration and then tracking the results throughout the deformation into the actual case. This provides the control needed in any numerical code to ensure reliable results. The resolution and accuracy of the calculations in the practical example given, and the relative ease with which they were performed, illustrates the engineering applicability of the method. It may finally also be noted that the derivation presented may be modified quite easily to include a uniform mean flow in the central passage. In fact, the numerical technique proposed for the dispersion relation is most suited for this as no eigenvalues, e.g., corresponding to possible hydrodynamic modes, will be lost.

ACKNOWLEDGMENTS

This study was financially supported partly by The National Board for Industrial and Technical Development (NUTEK), grant 90-01247 and partly by DUCAT, BE97-4109.

REFERENCES

1. P. M. MORSE 1939 *Journal of the Acoustical Society of America* **11**, 205–210. The transmission of sound inside pipes.
2. R. A. SCOTT 1946 *Proceedings of the Physical Society* **58**, 358–368. The propagation of sound between walls of porous material.

3. B. NILSON and O. BRANDER 1980/1981 *IMA Journal of Applied Mathematics* **26** and **27**. The propagation of sound in cylindrical ducts with mean flow and bulk-reacting lining.
4. A. CUMMINGS and I. J. CHANG 1988 *Journal of Sound and Vibration* **127**, 1–17. Sound attenuation of a finite length dissipative flow duct silencer with internal mean flow in the absorbent.
5. K. S. PEAT 1991 *Journal of Sound and Vibration* **146**, 353–360. A transfer matrix for an absorption silencer element.
6. V. TARNOW and C. POMMER 1988 *Journal of the Acoustical Society of America* **83**, 2240–2245. Attenuation of sound mufflers with absorption and lateral resonances.
7. K. S. PEAT and K. L. RATHI 1995 *Journal of Sound and Vibration* **184**, 529–545. A finite element analysis of the convected acoustic wave motion in dissipative silencers.
8. R. MITTRA and S. W. LEE 1971 *Analytical Techniques in the Theory of Guided Waves*. New York: The MacMillan Company.
9. M. ABRAMOWITZ and I. A. STEGUN 1965 *Handbook of Mathematical Functions*. New York: Dover Publications.
10. R. GLAV 1996 *Journal of Sound and Vibration* **189**, 123–135. The point-matching method on dissipative silencers of arbitrary cross-section.
11. P. M. MORSE and H. FESHBACH 1953 *Methods of Theoretical Physics*. New York: McGraw-Hill.
12. A. CUMMINGS and R. J. ASTLEY 1995 *Journal of Sound and Vibration* **179**, 617–646. The effects of flanking transmission on sound attenuation in lined ducts.
13. M. L. MUNJAL 1987 *Journal of Sound and Vibration* **116**, 71–88. A simple numerical method for three-dimensional analysis of simple expansion chamber mufflers of rectangular as well as circular cross-sections with a stationary medium.
14. R. MITTRA 1963 *Journal of Research of the National Bureau of Standards, D Radio Propagation* **67**, 245–254. Relative convergence of the solution of a doubly infinite set of equations.
15. C. VASSALLO 1985 *Theorie des guides d'ondes electromagnétiques 2*. Paris: Eyrolles.
16. G. A. GESELL and I. R. CIRIC 1992 *IEEE Transactions on Microwave Theory and Techniques* **41**, 484–490. Recurrence modal analysis for multiple waveguide discontinuities and its application to circular structures.
17. M. LEROY 1983 *IEEE Transactions on Antennas and Propagation* **AP-31**, 655–659. On the convergence of numerical results in modal analysis.
18. H. HUDDE and U. LETENS 1985 *Journal of the Acoustical Society of America* **78**, 1826–1837. Scattering matrix of a discontinuity with a nonrigid wall in a lossless circular duct.
19. M. ÅBOM 1989 *Journal of Sound and Vibration* **137**, 403–418. Derivation of four-pole parameters including higher order mode effects for expansion chamber mufflers with extended inlet and outlet.
20. S. IVANSSON and I. KARASALO 1993 *Journal of Sound and Vibration* **161**, 173–180. Computation of modal wavenumbers using an adaptive winding-number integral method with error control.
21. G. DAHLQUIST and Å. BJÖRK 1974 *Numerical Methods*. Englewood Cliffs, NJ: Prentice-Hall.
22. M. R. SPIEGEL 1968 *Mathematical Handbook of Formulas and Tables*. New York: McGraw-Hill.
23. R. GLAV 1992 *Proceedings ISATA 92*, 161–167. Computer simulation of sound propagation in inlet and exhaust systems.
24. M. E. DELANY and E. N. BAZLEY 1970 *Applied Acoustics* **3**, 105–116. Acoustic properties of fibrous absorbent materials.
25. A. CUMMINGS 1992 *Proceedings, 2nd International Congress on Recent Developments in Air- and Structure-Borne Sound and Vibration, Auburn, U.S.A.*, 689–696. Sound absorbing ducts.